Astron. Astrophys. 330, 1127–1135 (1998)

ASTRONOMY
AND
ASTROPHYSICS

Nanoparticles produced by Laser Pyrolysis of hydrocarbons: analogy with carbon cosmic dust

Nathalie Herlin[1], Isabelle Bohn[1], Cécile Reynaud[1], Michel Cauchetier[1], Aymeric Galvez[1,2], and Jean-Noël Rouzaud[2]

[1] Service des Photons, Atomes et Molécules, CEA-Saclay, F-91191 Gif-Sur-Yvette Cedex, France
[2] Centre de Recherche sur la Matière Divisée, 1B rue de la Férollerie, F-45071 Orléans Cedex, France

Received 22 April 1997 / Accepted 7 October 1997

Abstract. Infrared Laser Pyrolysis (IRLP) of gaseous molecules is a versatile method of synthesising a wide variety of nanopowders. The synthesis mechanism is based on condensation of heated gaseous precursors. This is the same mechanism as postulated for carbon dust formation in the envelopes of evolved C-rich stars. An advantage of this technique, in contrast with furnace- or plasma-heated gas phase techniques, is its well-defined reaction zone and its infrared heating process. Using hydrocarbon molecules C_2H_4 or C_4H_6 as precursors, a series of carbon-based nanoparticles have been obtained in synthesis conditions corresponding to a variety of reaction temperatures. The nanoparticles were characterised by Transmission Electron Microscopy (TEM) and infrared (IR) spectrometry. Both IR spectrum and molecular organisation appear to depend on the synthesis conditions: the lower the reaction temperature, the stronger the amorphous character and the more intense the IR bands. When present, IR bands are essentially due to aromatic CC and CH groups. Our experimental results are compared with results reported on other carbonaceous compounds and with astronomical observations.

Key words: molecular data – methods: laboratory – dust, extinction – Infrared: ISM: lines and bands – circumstellar matter

1. Introduction

It is generally agreed that carbon particles are produced in C-rich stellar envelopes from hydrocarbon molecules such as C_2H_2, and constitute a significant component of interstellar dust. The exact process is not well known, but development of a kinetic model to explain the formation of dust forms the research effort of several groups (Cherchneff et al. 1995; Frenklach and Feigelson 1996), and experimental data are needed. The infrared (IR) spectra observed in emission from a large number of circumstellar nebulae (Beintema et al. 1996; Justtanont et al. 1996; Sellgren et al. 1990 and references therein) give constraints on the optical properties of the carbon dust. It has been well established that the IR features are characteristic of C-H and C-C aromatic groups, with some contribution of aliphatic groups, and appear as broad and intense bands over a continuum. The ratio between these features and the continuum can change significantly from one object to another.

Several laboratories around the world are attempting to simulate cosmic dust condensation. Soots have been produced by hydrocarbon flame or arc-discharge in a neutral or hydrogenated atmosphere (Colangeli et al. 1995). Hydrogenated amorphous carbon films have been produced by plasma-assisted chemical vapour deposition (CVD) (Sakata et al. 1987) or by laser ablation of carbon targets in an H_2 atmosphere (Scott and Duley 1996). The large majority of the synthesised materials, however, have a strong aliphatic character and present a low features-to-continuum ratio in the IR range. Heat treatments increase the aromatic character of carbonaceous compounds (Dischler et al. 1983; Mennella et al. 1995) but lead to dehydrogenation and a subsequent increase of the continuum. The coal model (Papoular et al. 1989; 1996) is able to reproduce the diversity of the astronomical IR observations in feature positions and relative intensities (Guillois et al. 1996), but the possibility of formation of coal-like particles in cosmic environment is questionable.

Our aim is therefore to contribute to this field by using another synthesis method: the Infrared Laser Pyrolysis (IRLP) of gas phase molecular species. This method appears particularly interesting because it is based on homogeneous nucleation from vibrationally heated molecules. In this process, reactant gases are heated by IR laser radiation and decompose, causing aggregates to nucleate and grow rapidly without contribution of highly energetic or ionic particles. With cold, non-reactive chamber walls and a well-defined reaction zone, this process is inherently very clean. The small reaction volume and the ability to maintain steep temperature gradients allow precise control of the nucleation rate, growth rate, and exposure times. Since the reactants are dilute, the resulting powders are very fine, spherical, extremely pure, loosely agglomerated and nearly monodispersed in size. For example, in a typical IRLP SiC powder, the particles diameter exhibits a Gaussian distribution centred at

Send offprint requests to: Nathalie Herlin

Table 1. Experimental conditions of laser pyrolysis synthesis

Sample	Precursor	Flow (cm^3/min)	Pressure (Torr)	Laser power (W)	IR bands intensity
Powder A	C_2H_4	34	760	290	$--$
Powder B	C_2H_4	140	900	450	$-$
Powder C	C_2H_4	140	900	280	+
Powders D and E	C_2H_4	540	760	280	++
Deposit	C_4H_6	226	700	300	+++

25 nm, with a FWHM of 15 nm. The mean particle size usually varies from 10 to 100 nm, depending on the processing parameters. The high versatility of IRLP allows the production of a wide range of nanopowders including SiC, SiCN, SiCO, BN and fullerenes (Boulanger et al. 1995; Cauchetier et al. 1994; Ehbrecht et al. 1993; Herlin et al. 1996; Voicu et al. 1996). Their physical and chemical properties can be controlled by changing the molecular precursors and the synthesis parameters (Cauchetier et al. 1988). This contrasts with furnace-heated, rf-heated, and arc-plasma-heated gas-phase synthesis techniques in which the thermal profiles and reaction zones do not allow a precise process control (Cannon et al. 1982).

Therefore, laser pyrolysis appears useful to understand the process which converts C_2H_2 into carbon grains in the envelope of C-rich red giants. In this paper, the first results of IRLP synthesis of carbon-based particles are reported. The present work is focused on the IR spectroscopic properties as correlated with the growth mechanism. IR spectra, Electron Microscopy images as well as chemical analyses of the synthesised powders are reported. The influence of the synthesis parameters is discussed, and the results are compared to those of other solid models and to astronomical observations.

2. Experiment and results

2.1. Experimental procedure

The IRLP method is based on the interaction of an IR laser beam with a gaseous precursor which absorbs the laser radiation, leading to the formation of a flame where nanoparticles are synthesised. We now present a brief overview of the method; the experimental set-up has been described elsewhere in more detail (Cauchetier et al. 1988). The focused beam of a continuous wave CO_2 laser, emitting at 10.6 μm and delivering a power in the 200-1000 W range, crosses orthogonally a gaseous flow. The reaction occurs in a well defined zone usually called wall-less reactor. An inert gas such as argon carries the nanopowders away from the reaction zone. The powders are collected on a filter inside the extraction device about 40 cm away from the reaction zone, or deposited on a silicon substrate located right in the stream about 14 cm away from the reaction zone. When the deposits are observed between crossed polarisers in the latter case, we see a surface uniformly smooth and without irregularities at the micrometric scale. Profilometry measurements confirm the surface smoothness and yield the deposits thickness. It is linearly dependent on the duration of the experiment which is a clear indication of the stability of the experimental process.

The multiscale organisation of the as-formed powders is characterised by Transmission Electron Microscopy (TEM) and their elemental composition is obtained by classical chemical analysis (measurement of the CO_2 and H_2O quantities released after burning under oxygen atmosphere). The IR spectrum of each sample is recorded. An Infrared Fourier Transform (IFT) spectrometer is used with a Diffuse Reflectance (DR) cell for powders collected on the filter, and in transmission mode for deposits on silicon substrates. The DRIFT spectra are presented as $\log(1/R)$, where R is the diffuse reflectance, without any continuum subtraction. The transmission IR spectrum is presented after subtraction of the silicon substrate contribution but without continuum subtraction. Oxidation of the sample is easily detected by the presence of a shoulder in the IR spectra at 5.9 μm. Such a shoulder appears after a few hours of exposure to the atmosphere. To avoid oxidation of the samples, the experimental system, the IR spectrometer, and the glove-box used for sample storage, are kept in an argon atmosphere.

2.2. Influence of the synthesis parameters

The main synthesis parameters are the nature of precursors, reactor pressure, laser power and reactant flow rate. Change in the flow rate allows to change the residence time in the laser beam. Simple hydrocarbon molecules absorbing the 10.6 μm laser radiation have been chosen as the gas phase precursors, essentially C_2H_4 and C_4H_6. We have studied the influence of the following parameters: flow rate in the range 30-540 cm^3/min, pressure in the range 700-900 Torr and laser power in the range 280-450 W. All these parameters are expected to have a direct effect on the flame temperature. We have studied separately the effect of each parameter with the help of an optical pyrometer working in the range 1200-2500 K. We observed that the flame temperature increases when the flow rate decreases, i.e. when the residence time of the molecular species in the laser beam increases. The temperature also increases when the laser power or the pressure increases. For low temperatures ($\lesssim$1200 K), an estimation of the absolute value of the temperature is obtained by extrapolating an experiment performed at higher temperature ($\sim$1500 K), and the exact temperature is not well known. We have performed several synthesis experiments clearly exhibiting an evolution correlated to the variation of the experimental parameters. For clarity, in Table 1 we only consider experiments representative of the effect of the parameter variations, the others being intermediate cases. In Fig. 1 the DRIFT spectra of samples A and D are compared (see Table 1 for the synthesis conditions of the samples).

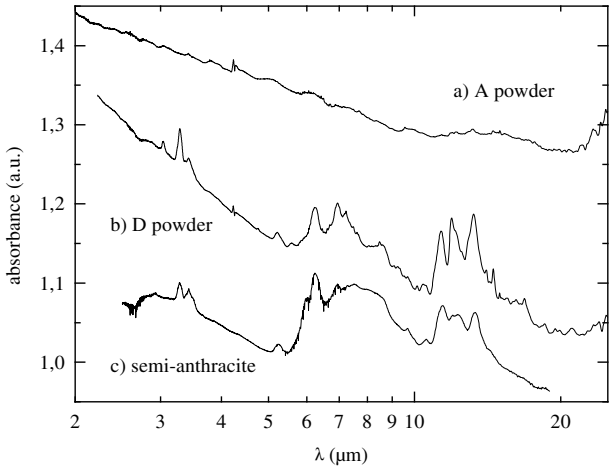

Fig. 1. DRIFT spectra recorded in the 2.5-25 μm range. The curves refer to a) powder A, b) powder D (see Table 1 for synthesis conditions), c) semi-anthracite coal, presented here for comparison. Data are given as log(1/R). In all spectra a small contribution at 4.25 μm due to CO_2 present in the spectrometer has been subtracted

The spectra are in most cases comparable to that of powder D (Fig. 1b), with more or less intense vibrational bands superimposed on a continuum decreasing at longer wavelengths. The bands indicate the presence of functional groups of C-C and C-H type (a detailed analysis of the IR spectra is presented below). However, in some cases such as that of sample A (Fig. 1a), the intensity of the bands can be very weak. Such a flat spectrum is considered as characteristic of amorphous carbon without heteroatoms or hydrogen (Papoular et al. 1996). In the last column of Table 1, the relative intensity of the characteristic IR bands compared to the continuum is described qualitatively.

The IR spectra show that, as expected, the flame temperature governs the synthesis. For instance, if we compare the synthesis conditions of samples D and A (respectively fourth and first line of Table 1), the only difference is in the lower flow rate (about a factor of ten) and therefore a higher flame temperature in A. A similar conclusion can be reached when pressure (sample B) or laser power (sample C) increases. Thus the characteristics of the IR spectra of the samples are directly correlated to the flame temperature: the synthesised powders exhibit the IR bands only if the flame temperature is approximately lower than 1200 K. In all cases, the yield of the reaction is weak (a few grams per hour) and decreases when the flame temperature decreases. The yield of this reaction is very low compared with that of other IRLP experiments. For example, when SiC is synthesised, the production rate is about 100 g/hour (Cauchetier et al. 1988). This is related to the much higher flame temperature in the latter case ($\sim$ 2100 K).

A chemical analysis has been done when the quantity of sample obtained was sufficient. For the particles exhibiting IR bands, the H/C atomic ratio is in the range 0.35-0.45. It is smaller than the ratio of 2 or 1.5 in the precursor molecules. For the powders synthesised at high temperature, the amount of hydrogen is smaller, as expected from the IR spectra. A small amount of O atoms ($\sim$ 3 %) is detected in the powders. This is due to the exposition of the particles to air, which cannot be avoided before chemical analysis and is responsible for the sample oxidation as noted in Sect. 2.1. (IR spectra reported in this paper have been recorded on samples preserved from the atmosphere).

2.3. TEM study of the samples: multiscale organisation

Most of carbons show a multiscale organisation: "structure" refers to the atomic scale and "microtexture" refers to sizes from nanometric to micrometric scales. The microtexture frequently results in the assembly of nanometric structural units. The multiscale organisation is studied by using various TEM modes (Oberlin et al. 1984) and especially the 002 lattice fringe mode permitting to image directly the profile of the aromatic layers. As observed previously in other IRLP chemical systems (Herlin et al. 1996), our IRLP carbon powders are mostly made of spherical particles with a mean diameter in the 20-40 nm range. The particles sometimes stick together in a chain-like manner. Despite the presence of a single precursor introduced in the reactor, the powders are heterogeneous structurally (coexistence of amorphous and turbostratic carbons) and microtexturally (blends of concentric, porous and lamellar particles). The low flame temperature (about 1200 to 1500 K) of the IRLP synthesis in the present case can explain this heterogeneity which is not observed in usual IRLP conditions.

The two most frequently observed organisation types are illustrated in Fig. 2 with the help of samples B (top) and E (bottom) (see Table 1 for their synthesis conditions) and are:

– a concentric microtexture (top of Fig. 2), due to the concentric orientation of polyaromatic Basic Structural Units (BSU) (stacks of 2-3 aromatic layers, about 1 nm in diameter). The size of such particles is frequently a few tens nanometers in diameter (about 40 nm for sample B, Fig. 2). Their structure is turbostratic as demonstrated by the electron diffraction pattern (insert of Fig. 2): presence of a 002 ring and hk band, without hkl reflections characteristic of a triperiodic order (Oberlin et al. 1984; Oberlin 1992). The microtexture of these particles is similar to the classical onion-like structure proposed by Heidenreich et al. (1968) for the carbon blacks obtained by incomplete combustion of hydrocarbons. Our concentric nanoparticles are, however, frequently embedded in an amorphous phase or surrounded by a skin of amorphous carbon.

– an amorphous-like carbon (bottom of Fig. 2), i.e. without any clearly detectable polyaromatic Basic Structural Units (BSU) as shown by the 002 Lattice Fringe TEM mode. Indeed the electron diffraction pattern is characteristic of an amorphous carbon: only broad, diffuse and faint 10. and 11. bands are visible (insert of Fig. 2). The corresponding periodicities (2.1 and 1.2 Å) are attributed to two inter-row distances inside biperiodical polyaromatic structures. This order is, however, only local (subnanometric isolated graphene-like layers). It is disrupted by numerous defects such as tetrahedral carbon atoms (sp^3), hydrogen atoms and heteroatoms. Consequently, such aromatic-like structures are randomly distributed and their stacking is prevented (no 002 reflection in the pattern) giving a quasi-

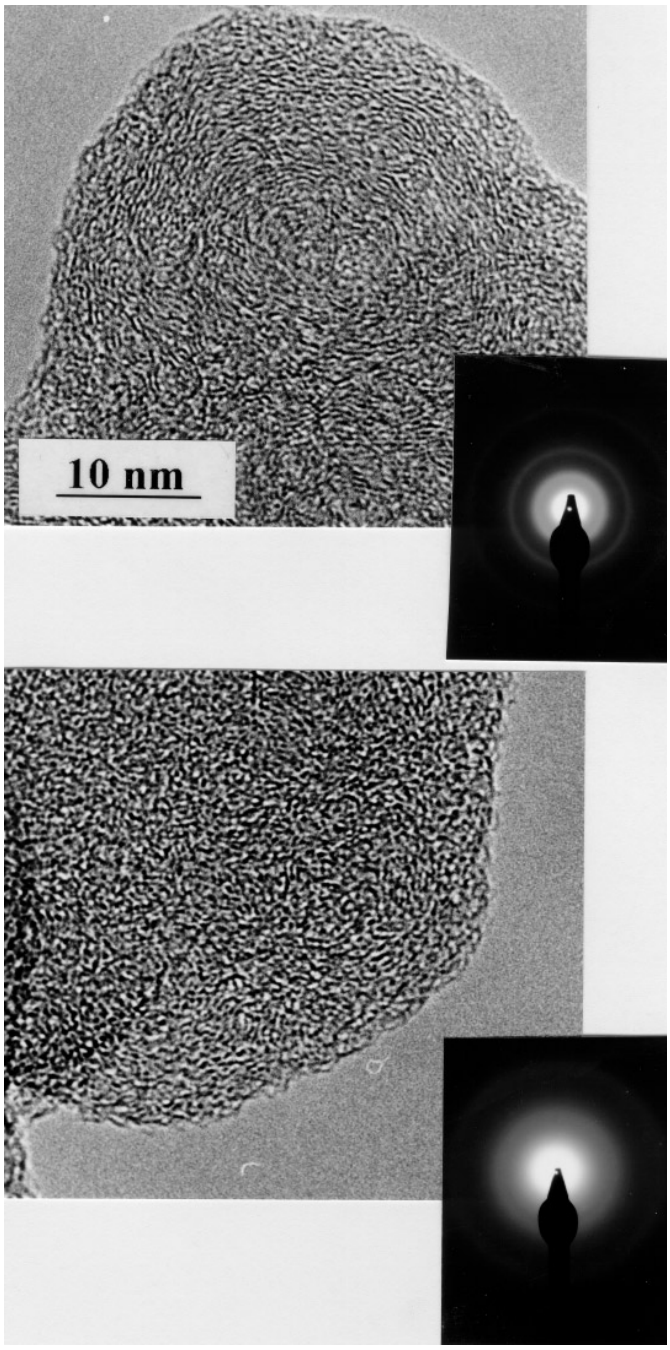

Fig. 2. High Resolution TEM images and Electron Diffraction Patterns (inserts) of infrared laser pyrolysis samples: concentric microtexture in sample B (top); amorphous phase in sample E (bottom)

amorphous structure. The order is lower than for the polyaromatic BSU formed by 2-3 nanometric layers stacked in parallel (turbostratic stacking) (Oberlin et al. 1984; Oberlin 1992). The mean size of the particles is also about 40 nm in sample E (Fig. 2). The semi-quantitative data resulting from this TEM characterisation are given in Table 2. At present, we only evaluate the proportions of the different types of carbon organisation as absent, traces, present and abundant. A more quantitative description can be obtained by using low magnification (x 20 000) 002 dark field images for particles counting. This detailed approach is in progress. Globally, sample B is the best organised sample of this series, whereas sample E is mainly amorphous, and the deposit quite amorphous. The correlation with the IR results reported above shows that the lower the flame temperature, the more intense the IR bands and the more amorphous the organisation. In addition, the amount of concentric orientation of polyaromatic BSUs can be tentatively correlated to the intensity of the IR continuum, since the samples showing the highest IR continuum show such concentric orientation. Such IR continuum is probably due to the IR tail of the electronic absorption band commonly observed in non-crystalline small-gap semiconductor (Robertson 1992).

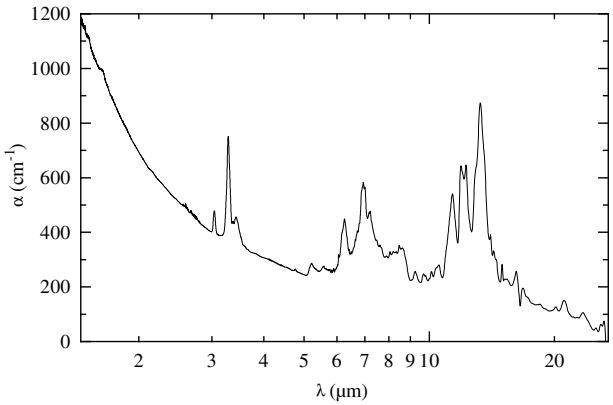

Fig. 3. Spectral absorbtivity of deposited sample measured in the transmission mode in the 1.5-25 μm range ($\alpha = \ln(I_0/I)/d$, where d=17 μm is the deposit thickness, and I the transmitted IR intensity)

Table 2. Semi-quantitative TEM data analysis. The synthesis conditions are given in Table 1

Sample	Amorphous carbon	Concentric phases
powder B	traces	abundant
powder E	abundant	present
deposit	abundant	absent

2.4. IR spectroscopy

Fig. 3 presents the IR spectrum of the IRLP deposit. This deposit appears rather homogeneous and smooth with a thickness of 17 μm. These observations lead us to assume that it is a compact layer of nanoparticles and to present its IR spectrum in units of spectral absorbtivity. The comparison of the spectra of sample D and deposit presented in Fig. 1 and Fig. 3 respectively, shows that the deposit and the powder synthesised in rather similar conditions are similar from a spectroscopic point of view (positions and bandwidths). Therefore, deposition does not induce a modification of the nanoparticles. This is compatible with recent experiments on IRLP silicon particles deposition (Ehbrecht et al. 1997). Also, keeping in mind that in Fig. 3 only the contribution of the silicon substrate has been subtracted from the recorded spectrum, the reported result gives the absolute value

Table 3. IR features (in μm) present in deposited IRLP sample and coal (present work) compared to the main infrared UIBs (Beintema et al. 1996).

Deposited sample	Coal (semi-anthracite)	UIB SWS (NGC 7027)	Assignment
	2.92		OH stretch in coal
3.04			CH acetylenic stretch
3.28	3.28	3.287	CH aromatic stretch
3.37	3.38	3.398	CH aliphatic stretch(CH_3 antisym)
3.43 (broad)	3.43		CH aliphatic stretch(CH_2 antisym)
		3.467	CH aliphatic stretch
	3.51	3.518	CH aliphatic stretch(CH_2 sym)
4.76			C≡C stretch of alkynes
5.22	5.25	5.234	C=C stretch of allenes
5.6		5.650	CH out of plane summation bands
	5.98		C=O stretch in coal
6.25	6.25	6.219	C=C aromatic stretch (quadrant)
6.94	6.93	6.924	CH aliphatic deformation (CH_2 and CH_3 antisym)
7.00			and C=C aromatic stretch (semicircle)[a]
7.20	7.27		CH aliphatic deformation (CH_3 sym)
7.61	7.52	7.594	CC / CH aromatic
		7.815	
	8		C-O in coal
8.46 and 8.63	8.6	8.585	CH aromatic deformation in-plane
	9.66		minerals in coal
10.54	10.58	10.44	CH vinyl deformation
		11.05	
11.36	11.4	11.22	CH aromatic deformation out of plane solo
		11.76	
11.92	11.95	11.95	CH aromatic deformation out of plane
12.27	12.3 (broad)		duo and trio
		12.73	
13.27	13.33	13.58	CH aromatic deformation out of plane quarto
		17.03	
		17.86	
21.1			ring deformation
23.4			ring deformation

[a] strongly mixed with in plane CH deformation

of the absorption coefficient of sample. It appears that the bands are intense compared to the continuum. For example, the band over continuum ratio is equal to 2 at 3.28 μm. The peak positions of the most intense IR bands for the deposited sample are reported in Table 3. Most of the signatures can be assigned to CH and CC bonds, as it has been well established for hydrogenated carbonaceous compounds (see for example Dischler et al. 1987; Lin-Vien et al. 1991). A detailed assignment of the different bands is given in the last column of Table 3. As common to several carbon based samples, the IR spectrum of the IRLP deposit is essentially composed of 3 groups of bands. The first group, in the range 3-4 μm, corresponds to the C-H stretching vibrations and is detailed in Fig. 4. The second group between 5 and 10 μm is a composite massif discussed in details below. The third group (between 10 and 15 μm) is characteristic of the aromatic C-H bending modes. The strong aromatic character of this deposit is evidenced by the high intensity of the peaks in this last region. In fact, most of the bands present in the spectrum can be assigned to aromatic modes:

– In the first group (Fig. 4), the highest contribution is always at 3.28μm and is attributed to the C-H stretching mode of aromatic compounds. This peak presents a shoulder at short wavelengths indicating a composite band ($FWHM$ = 0.06 μm). It is difficult to deduce more information on the aromatic chemical environment from this spectral region.

– In the second group, the C=C ring stretching modes (6.25 and 6.94 μm) and C-H in plane bending modes (8.46 and 8.63 μm) of aromatic compounds are observed. The band at 7.61 μm is also attributed to aromatic structures despite the great diversity of assignment proposed for bands in this spectral region in the literature (see the discussion in the paper of Sellgren (1990)). For example, the 7.7 μm band is sometimes attributed to an oxygenated group (Charcosset 1990; Sakata et al. 1987). This is not possible in the present case since the sample is oxygen-free (the lack of feature due to C=O bonds near 5.9 μm indicates that the deposit contains very few oxygenated bonds if any).

– The third group gives the most precise information on the aromatic compounds present in the sample. These bands are

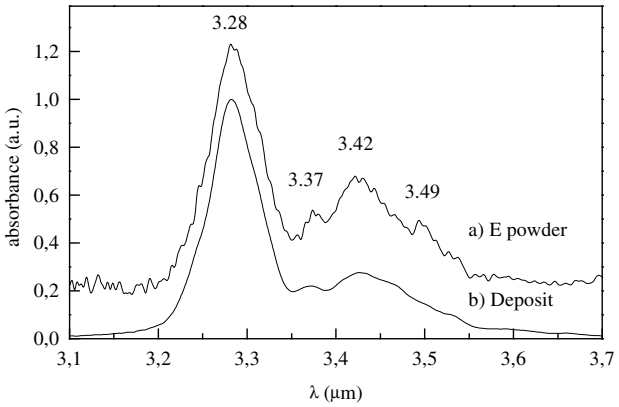

Fig. 4. C-H stretch region (3.1-3.6 μm) of the IR spectrum of a) powder E, b) the deposit, after linear background subtraction

due to the various C-H out-of-plane vibrations and exhibit always a strong intensity (see for example Lin-Vien et al. 1991 and references therein). Their wavelengths strongly depend on the substitution degree and on the position of the substituents on the ring, and these bands are therefore very specific of the aromatic structures. Three intense features are observed. The band at 11.36 μm is attributed to the C-H vibration of a lone H. The next feature exhibits two maxima at 11.92 and 12.27 μm: they are due to two or three adjacent H in a substituted ring. The last band at 13.27 μm which is the most intense corresponds to C-H vibrations in compounds with four adjacent H on a ring. Since this corresponds to di-substituted aromatic rings in terminal position, the 13.27 μm band can be associated with the presence of small aromatic units. Binary combinations and overtones of C-H out-of-plane modes (summation-type bands) can be responsible for the weak structure observed around 5.6 μm (Lin-Vien et al. 1991).

The other bands family observed in all spectra corresponds to the aliphatic species. They contribute to the band around 3.4 μm, due to the C-H stretch, as well as to the 6.94 and 7.20 μm bands attributed to C-H deformation modes. The band at 3.43 μm (Fig. 4) is a composite band with a tail extending up to 3.6 μm and presenting some variation over the explored experimental conditions as evidenced by the comparison of the spectra of the deposit and the E powder in Fig. 4. The band intensity can change slightly with the synthesis conditions but it is always weaker than the 3.28 μm aromatic band. The band maximum is always between 3.42 and 3.43 μm. A structure at 3.37 μm is systematically observed, whereas the shoulder at about 3.5 μm is not always present. All these bands are due to C-H stretching modes but correspond to various aliphatic groups in various environment (Table 3).

Several minor bands are observed in the spectrum. The band at 10.54 μm is attributed to olefinic C-H out of plane deformations. The band at 5.22 μm is tentatively assigned to C=C=C cumulenes (Balanzat et al. 1996). Alkyne groups (-C≡C-H) are responsible for the weak bands at 3.04 μm and 4.76 μm which correspond to the C-H and C≡C stretching, respectively. Alkynes are thermodynamically more stable at high temperature and acetylene is the dominant molecule formed in flames and in the outflow of carbon-rich giant red stars (Frenklach and Feigelson 1996). It is therefore not surprising to observe that the IRLP samples retain alkyne groups. Subsequent short heat treatment at 500 K leads to the disappearance of both alkynes bands, in agreement with results reported by Dischler (1987) for carbon compounds.

Multiple narrow lines with low intensity are present in three regions of the spectrum: between 5.7 and 6 μm, between 8.0 and 8.4 μm, and between 9.1 and 10.3 μm. They are assigned to combination modes of CH out of plane deformations, to CH in plane deformations, and to CH deformations in vinyl or phenyl groups respectively. Finally, above 15 μm, several lines appear at 15, 16.2, 18.5, 20.2, 21.1 and 23.4 μm, the two last lines being the most intense. Assignment of these lines to aromatic ring deformation modes is the only one compatible with the whole spectrum.

3. Discussion

3.1. Comparison with natural materials: coal

The comparison with a coal sample was chosen in this study not only because coals are very well documented materials (Charcosset 1990) but also since coals exhibit structures from purely aromatic to a mixture of aromatic and aliphatic (Guillois et al. 1996). Comparing with different coals, the synthesised powder appears to be rather similar to a semi-anthracite coal, such as Escarpelles (Charcosset 1990), both in its C/H atomic ratio (0.40) and in its IR spectrum (Fig. 1). This similarity is interesting because the spectra of this type of coal have been shown to give the best agreement with the emission spectra observed from protoplanetary nebulae (Guillois et al. 1996). Moreover, this similarity stresses the universality of the carbonisation process, since coals are formed in a very different way, namely by condensation of organic matters in the earth subsoil.

If we compare the spectra of IRLP samples with those of semi-anthracite (Fig. 1), the same 3 groups of bands are observed. In both spectra, the first group around 3.3 μm and the third group between 11 and 14 μm are composed of the same lines located at the same spectral positions and with similar bandwidths. In those two groups, the only differences are in the intensity ratios. The 3.28 μm (aromatic C-H) over the 3.4 μm (aliphatic C-H) band intensity ratio is higher in the IRLP sample than in coal. In the third group, in coal the 11.4 μm band, due to a solo H atom attached to an aromatic ring, is the most intense, whereas in the IRLP sample, the most intense is the 13.27 μm band, mostly due to 4 adjacent H atoms. This implies that the IRLP sample is more aromatic and is probably made up of smaller units than semi-anthracite coal. For the second group of bands (5 to 10 μm) both samples show a similar general trend, with maxima at 6.25 and 6.94 μm. However, some differences appear: in the IRLP sample, the bump around 8.6 μm rises distinctly over the continuum but the intensity in the 7.5-8 μm range is relatively low. This low intensity can be related to the absence of oxygen in the IRLP sample, as evidenced by the absence of the 2.9 and 5.9 μm bands corresponding re-

spectively to OH and C=O bonds, which are present in coal. The absence of oxygen, however, cannot completely explain this difference, since the massif at 7-8 μm is still present with a high relative intensity in the spectrum of anthracite coals (Guillois et al. 1996) which exhibit lower hydrogen and oxygen content (Charcosset 1990). Anthracite coals are still more evolved than semi-anthracite coals and incorporate polyaromatic BSUs (see above in Sect. 2.3.) with better local organisation (Rouzaud & Oberlin 1990). It has, moreover, been shown that such a 7.7 μm band can be connected with the creation of a reticulated network in carbonaceous compounds (Balanzat et al. 1996). The weakness of the 7.61 μm band in the IRLP sample is therefore tentatively related to the lack of polyaromatic BSUs as reported above from the TEM study (Sect. 2.3.).

3.2. Comparison with synthesised materials

Among the different samples described in the literature (see for example Figs. 6 and 7 in Papoular et al. 1996), the oxidised f-QCC films (Sakata et al. 1987) appear to be the most similar to IRLP samples if we consider the IR spectra. In the IRLP case, however, it is not necessary to refer to an oxidation process in order to explain the 8.6 μm band intensity as in the case of the oxidised f-QCC samples (Sakata et al. 1987). The major difference between the spectra is the aromatic character which appears much more marked in the IRLP sample than in the f-QCC films, as shown by the 3.28 μm over 3.4 μm band ratio. The same conclusion can be reached by comparison with HAC samples spectra (Scott and Duley 1996). It is interesting to note that the precise positions of the aliphatic bands given in this paper (3.38, 3.42, 3.48 μm) are very close to the positions reported here (Fig. 4).

To our knowledge, the combustion method (Colangeli et al. 1995) was previously the only case where a man-made material with aromatic character has been obtained (3.3 μm to 3.4 μm band ratio >1). The band-over-continuum ratio, however, is very weak (1.01 at 3.3 μm, which means that the intensity in the band is only 1% of the total intensity) in the combustion sample while it reaches a value of 2 in the IRLP deposit. Such a high value is unique for a man-made laboratory sample. An aromatic character is usually achieved by annealing aliphatic materials (Dischler et al. 1983; Mennella et al. 1995), but heat-treatments lead to carbonisation of the samples and to decrease of the aromatic band over continuum ratio. The hydrogen content should play an important role in determining the band intensity since most of them are due to C-H bonds. Comparison with the TEM studies of other artificial materials (Colangeli et al. 1995; Koike et al. 1994) shows that the IRLP deposit is the least-organised sample. It is consistent with the observation that the intensity of the IR bands and the molecular organisation are correlated.

3.3. Comparison with astronomical data

We chose to compare our results with the recent data on circumstellar envelopes and planetary nebulae obtained with ISO by Beintema et al. (1996). The peak positions quoted for the well-studied planetary nebula NGC 7027 are reported in Table 3 for easier comparison. For the major bands, the bandwidths and peak intensities of the IRLP deposit are compared to those of NGC 7027 and of the pre-planetary nebula HR 4049 in Table 4. Bandwidths can be measured only for the isolated bands such as the 3.3, 6.2 and 11.3 μm bands and can be evaluated for the 8.6 μm shoulder. Generally speaking, the IRLP sample bands are broader than the observed bands, the difference being the smallest in the case of the 6.2 μm band. An encouraging point is that the shape of the IRLP 8.6 μm band is very similar to the shape of the observed band.

Four of the main mid-IR bands (also UIBs for Unidentified IR bands), at 3.3, 6.2, 8.6 and 11.3 μm, are clearly observed in the IRLP samples (Fig. 3). By contrast, around 7 μm the IRLP spectrum has intense 6.9 μm band which is weak in NGC 7027, while the 7.61 μm band is weak compared to the intense 7.6-7.8 μm UIBs seen in the astronomical objects. In the latter the 7.7 μm band is the strongest one in the 6-9 μm massif, while it is the opposite in the IRLP sample (Table 4). If the 7.7 μm band is attributed to an extended aromatic network, its weakness may be related to the limited number of extended polyaromatic units in the IRLP samples as discussed above. Another explanation can be found in the absence of heteroatoms in our sample, since heteroatoms are expected to enhance the intensity of this band by breaking its symmetry (Sellgren 1990). The intensity of the 3.3 μm band relative to the 6.2 μm one is higher in the IRLP sample than in the observations (Table 4), but most of the difference is due to the limited temperature of the grain in the astronomical objects. I must also be noted that the observed band over continuum ratio for NGC 7027 is about 4 at 3.28 μm while it is 2 in the IRLP deposit.

The 3.28, 6.25 and 8.63 μm bands of IRLP samples are very close in position to the astronomically observed ones. The 11.3 μm is slightly shifted towards longer wavelengths in the IRLP sample (11.36 μm) compared to the observed value of 11.22. The limited size of the aromatic units in the IRLP samples can explain this difference since this band shifts towards shorter wavelengths from semi-anthracite to anthracite coals, i.e., when the samples become more aromatic and organised (Guillois et al. 1996).

As for the minor UIBs seen in the astronomical sources, most of them are exhibited by the synthesised sample. This is the case for the 3.4 μm group of bands, as well as for the 5.23, 5.65, and 10.44 μm bands, which are obtained with a correct ratio compared to the major band at 6.22 μm. This is also the case for the astronomically observed 6.92, 11.95 and 13.58 μm bands, which are found in the IRLP sample (bands at 6.94, 11.92 and 13.27 μm, respectively) but with very different relative intensities. However the 11.05, 11.76 and 12.73 μm minor UIBs are not clearly present in IRLP spectra. The 11.05 μm band has recently been shown to be spurious (Shipman et al. 1997), the 11.76 μm is very weak and the 12.7 μm band is not always correlated with the UIBs. Generally speaking, the group of bands between 10 and 14 μm often appears in astronomical observations as a plateau strongly dominated by the 11.3 μm band. Such a behaviour can be found only in anthracite coal (Guillois et al.

Table 4. Comparison of bandwidths and intensities of the IRLP deposit to the main mid-IR bands (from Beintema et al. 1996).

	NGC 7027[a]		HR 4049[a]		IRLP deposit	
Position(μm)	width(μm)	intensity(Jy)	width(μm)	intensity(Jy)	width(μm)	intensity(cm^{-1})
3.3	0.037	19.8	0.045	5.13	0.06	372
6.2	0.150	51.6	0.165	14.5	0.20	216
7.7	0.554	75.1	0.496	23.56	$-$[b]	120
8.6	0.320	42.7	0.25	12.5	~ 0.4	120
11.3	0.215	238	0.152	15.9	0.46	332

[a] from Beintema et al. 1996

[b] band not isolated enough for such measurement (see Fig. 3)

1996) among all the model materials studied up to now and our IRLP materials do not match them.

Finally, it is interesting to discuss the features present in the 21 μm range. These bands have attracted much attention since they appear in several astronomical spectra, often correlated to the UIBs as in carbon-rich post-AGB objects (Justtanont et al. 1996). In such objects, five bands are quoted at 20.24, 20.59, 21.03, 22.41 and 23.06 μm respectively. IRLP sample bands at 20.2, 21.1 and 23.4 μm are in relatively good agreement with three of them.

4. Conclusion

The results presented here indicate that infrared laser pyrolysis is a useful method in order to simulate the formation of carbon cosmic dust. Varying the reaction temperature in the gas phase allows the formation of powders with various properties. At high temperature, the powders appear quite organised with concentric microtexture and their IR spectra show only a continuum without noticeable features, which indicates a low hydrogen content. At lower reaction temperature ($<$1200 K), no organisation is detectable by TEM analysis, indicating a completely amorphous phase, but the IR spectrum presents a low continuum and strong signatures mainly due to CC and CH aromatic groups. The more amorphous the structure, the more intense the IR bands, which can be understood in terms of H content. The possibility given by the laser pyrolysis of controlling the flame temperature allows to retain a high quantity of hydrogen atoms in the sample.

The IRLP samples are of interest as models for carbon cosmic dust for several reasons:

i) The particles are synthesised below 1200 K by a homogeneous chemical process from heated molecules in the gas phase. The synthesis temperature and the formation mechanism appear compatible with the conditions in evolved C-rich stars envelopes.

ii) The particles are of nanometric size (a few tens nanometers), which is in the size range of cosmic dust (from about one to a hundred nanometers).

iii) The band over continuum ratio is high, a condition which is required to reproduce the observations in most of the cases.

iv) From a spectroscopic point of view, IRLP samples exhibit both aromatic and aliphatic IR bands, with a domination of the aromatic bands, as in the astronomical observations.

However the IRLP samples exhibit an intensity of the 6.9, 12.2 and 13.3 μm minor UIBs higher than observed in circumstellar material, as it is the case for many model compounds. Furthermore, the 7.7 μm band is weaker. We have tentatively interpreted this weakness by the limited size of the polyaromatic units. One should also remember the role of heteroatoms to increase the 7.7 μm band intensity. Further studies are necessary to answer these questions.

We are planning new synthesis with more refined control of the parameters. The role of heteroatoms such as N, O or Si, which are present in circumstellar envelopes, will be studied by changing the gaseous precursors. The samples will be submitted to annealing and irradiation under controlled atmosphere, which can simulate also the interstellar processes. The studied spectral range will be extended towards the UV.

Acknowledgements. We are very grateful to E. Balanzat, J. Conard, O. Guillois, I. Nenner and particularly to R. Papoular for fruitful discussions. Special thanks are due to P. Viel for interest in this work and samples thickness measurements. This work is supported by the CNRS/CEA/CNES Programme National "Physicochimie des Molécules et Grains Interstellaires".

References

Balanzat E., Bouffard S., Bouquerel A., Devy J. and Gaté Chr. 1996, Nucl. Instr. and Meth. B 116, 159

Beintema, D.A., Van Den Ancker, M.E., Molster F.J., Waters L.B.F.M., Tielens A.G.G., Waelkens C., de Jong T., de Graauw Th., Justtanont K., Yamamura I., Heras A., Lahuis F. and Salama A. 1996, A&A 315, L369

Boulanger L., Andriot B., Cauchetier M. and Willaime F. 1995, Chem. Phys. Lett. 234, 227

Cannon W., Danforth S., Flint J., Haggerty J. and Marra R. 1982, J. Am. Ceram. Soc. 65, 324

Cauchetier M., Croix O. and Luce M. 1988, Advan. Ceram. Mater. 3, 548

Cauchetier M., Croix O. Herlin N. and Luce M. 1994, J. Am. Ceram. Soc. 77, 993

Charcosset H. 1990, Advanced methodologies in coal characterization, Coal science and Technology series vol. 15, Elsevier

Cherchneff I. 1995, Ap&SS 224, 379

Colangeli L., Mennella V., Palumbo P., Rotundi A. and Bussoletti E. 1995, A&A 303, 976

Dischler B., Bubenzer A. and Koidl P. 1983, Solid State Comm. 48, 105

Dischler B. 1987, E-MRS Meeting 17, 189

Ehbrecht M., Faerber M., Rohmund F., Smirnov V.V., Stelmach O. and Huisken F. 1993, Chem. Phys. Lett. 214, 34

Ehbrecht M, Kohn B., Huisken F. Laguna M. and Paillard V. 1997, to be published in Phys. Rev. B

Frenklach M. and Feigelson E. 1996, Proceedings of the Symposium of the Astronomical Society of the Pacific "From Stardust to Planetesimals", Santa-Clara.

Guillois O., Nenner I., Papoular R. and Reynaud C. 1996, ApJ 464, 810

Heidenreich R.D., Hess W.H. and Ban L.L. 1968, J. Appl. Cryst. 1, 1.

Herlin N., Armand X., Musset E., Martinengo H., Luce M. and Cauchetier M. 1996, J. European Ceram. Soc. 16, 1063

Justtanont K., Barlow M.J., Skinner C.J., Roche P.F., Aitken D.K. and Smith C.H. 1996, A&A 309, 612

Koike C., Kaito C. and Shibai H. 1994, Mon. Notes R. Astron. Soc. 268, 321

Lin-Vien D., Colthup N.B., Fateley W.G. and Grasselli J.G. 1991, The Handbook of infrared and Raman characteristic frequencies of organic molecules, Academic Press, Inc.

Mennella V., Colangeli L., Bussoletti E., Monaco G., Palumbo P. and Rotundi A. 1995, ApJS. 100, 149

Oberlin A., Goma J. and Rouzaud J.N. 1984, Techniques d'étude des structures et textures (microtextures) des matériaux carbonés, J. Chim. Phys. 81, 701-710.

Oberlin A. 1992, in Chemistry and Physics of Carbon Vol. 22, ed. P.A. Thrower M. Dekker New-York, p. 1

Papoular R., Conard J., Guiliano M., Kister J. and Mille G. 1989, A&A 217, 204

Papoular R., Conard J., Guillois O., Nenner I., Reynaud C. and Rouzaud J.N. 1996, A&A 315, 222

Robertson J. 1992, Phil. Mag. B 66, 199

Rouzaud J.N. and Oberlin A. 1990, chapter 17 in Charcosset H. (1990)

Sakata A., Wada S., Onaka T. and Tokunaga A. 1987, ApJ 320, 63

Scott A. and Duley W. W. 1996, ApJ 472, L123

Sellgren K. 1990, Dusty objects in the universe, Bussoletti E. and Vittone A. Eds., Kluwer Academic Publishers

Shipman R., Beintema D. and Waters R. 1997, ISO Note.

Voicu I., Armand X., Cauchetier M., Herlin N. and Bourcier S. 1996, Chem. Phys. Lett. 256, 261

This article was processed by the author using Springer-Verlag LaTeX A&A style file *L-AA* version 3.